EPSC Abstracts
Vol. 10, EPSC2015-37, 2015
European Planetary Science Congress 2015

The young surface of (50000) Quaoar

M. A. Barucci (1), C. M. Dalle Ore (2), D. Perna (1), D. P. Cruikshank (2) , A. Doressoundiram (1) , A. Alvarez-Candal (3), E. Dotto (4), and C. Nitschelm (5)

(1) LESIA – Observatoire de Paris, CNRS, UPMC Univ. Paris 06, Univ. Paris-Diderot, 5 place J. Janssen, 92195, Meudon, France (antonella.barucci@obspm.fr / Fax : +33 145077144), (2) NASA Ames Research Center, Mail Stop 245-6, Moffett Field, CA 94035, USA, (3) Observatorio Nacional, Rio de Janeiro, Brazil, (4) INAF-Osservatorio di Monteporzio, Roma, Italy, (5) Unidad de Astronomía, Facultad de Ciencias Básicas, Universidad de Antofagasta, Antofagasta, Chile

Abstract

We present new continuous spectra from visible to near-infrared (0.3-2.3 μm) obtained with the X-Shooter instrument at the VLT-ESO at four different epochs on the surface of Quaoar. The data are complemented by previously published photometric observations obtained in the near-infrared (3.6, 4.5 μm) with the Spitzer Space Telescope. Spectral modeling was performed for the entire wavelength range by means of a code based on the Shkuratov radiative transfer formulation and using an updated value of albedo obtained from Herschel observations.

1. Introduction

(50000) Quaoar is one of the largest classical transneptunian objects in a binary system, with a recent diameter determination of 1036±31 km and an albedo of 12.7% [1] obtained with Herschel observations together with revised Spitzer data. Quaoar is also a very red object, classified as RR type [2] for its red spectral slope. It also appears to be rich in more complex irradiation products.

New observations were performed in August 2013 at the ESO-VLT using a new generation spectrograph X-Shooter recording simultaneously from ultraviolet to near-infrared (0.3-2.3 μm) wavelenghts. The data obtained at different rotational phases are complemented by previously published photometric data [3] in the near-infrared (at 3.6, 4.5 μm) obtained with the Spitzer Space Telescope. Along with the updated visible albedo [1] the Spitzer data provide an extra set of constraints in the model calculation process. For the new four spectra we perform spectral modeling first of the wavelength range from 0.3 to 2.3 μm and then adding the Spitzer data for extra contraints. We make use of a code based on the Shkuratov et al. [4] radiative transfer formulation of the slab model.

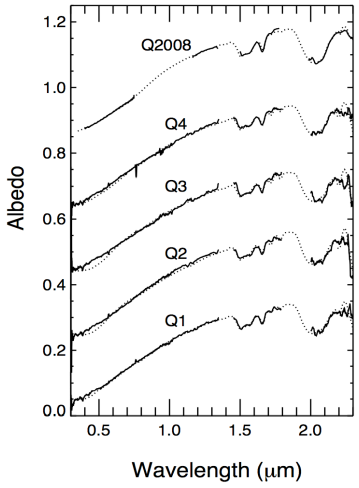

Figure 1: Five spectra of (50000) Quaoar (solid lines) are shown with their corresponding spectral models (dotted lines). Spectra labeled Q1 through Q4 are newly obtained, while Q2008 is from previous observations [3]. The top four spectra have been shifted by +0.2, +0.4, +0.6 and +0.8 units for clarity.

2. Observations and analysis

We present new visible to near-infrared (0.3-2.3 μm) spectral data obtained with the X-Shooter at the VLT-ESO at four different epochs on the surface of Quaoar. The newly obtained data cover about 40% of the object's rotation, with the assumption that the rotational period is 8.84 hrs [5]. The observations show a strong similarity as reported in Fig. 1 (Q1-Q4 spectra) which implies homogeneity of the surface composition on one hemisphere of Quaoar. This is also confirmed by the best fitting models calculated with a radiative transfer code [4]. Spitzer IRAC data [3] were also included with the new spectral data to better constrain the composition of the surface (Fig. 2). The best fitting model is reported in Table 1.

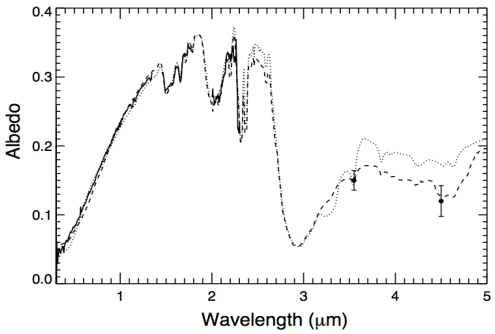

Figure 2: Spectrum of Quaoar (Q2, solid line) with Spitzer photometry (black dots) and corresponding best fitting spectral model (dashed line, parameters are listed in Table 1) that includes CO diluted in N_2 and CO_2. The best fitting model for the spectral dataset, without CO and CO_2, is also shown for comparison (dotted line).

6. Conclusions

Quaoar's visible spectral red slope is best matched by the inclusion of Triton and Titan tholin. H_2O ice in its crystalline phase is also clearly present. Quaoar's surface composition is partly inferred from the shifts of the CH_4 bands, as expected when this material is embedded in a N_2 matrix. Like CO in N_2, CO_2 is also included in the model only as an upper limit necessary to match the data at the two Spitzer bands. The comparison between the old Q2008 model and the new ones offers further evidence in favor of the presence of diluted CO and CO_2 on Quaoar. In the old model very small H_2O ice grains had to be adopted to fit the Spitzer data. With the inclusion of CO in N_2 and CO_2 this is no longer necessary.

The presence of crystalline H_2O ice and NH_4OH on the surface of Quaoar, may indicate an efficient renewal mechanism in favor of the hypothesis of a young surface. Numerical simulations [6] describing the thermal evolution of TNOs as function of the intensity of radiogenic heat, predicts the possible presence of cryovolcanism on Quaoar. Alternatively, crystalline H_2O ice could be the product of impact gardening and NH_4OH could be seeping up to the surface of Quaoar by a diffusive mechanism.

The spectrum of Quaoar is consistent with that of a cold object slowly losing the last of its volatile ices by escape to a tenuous atmosphere.

Table 1: Best fit of the Quaoar spectrum and the Spitzer data

Components	Q2+Spitzer
Titan tholin in CH_4	0.13
Triton tholin in CH_4	0.09
Triton tholin in H_2O	0.08
H_2O cryst (40K)	0.07(18)
C_2H_6 in N_2	0.02(31)
Triton tholin	0.36(7)
N_2 (36-60K)	0.03(1610)
CH_4 in N_2	0.21(80)
CO in N_2	0.05(150)
AC	0.11(20)
CO_2	0.04(100)
NH_4OH	0.12(65)

References

[1] Fornasier, S., Lellouch, E., Muller, T. et al. 2013, A&A 555, A15
[2] Barucci, M. A., Belskaya, I. Fulchignoni, M. et al. 2005, AJ, 130, 1291
[3] Dalle Ore C.M., Barucci, M. A., Emery, J.P. et al. 2009, A&A, 501, 349
[4] Shkuratov, Y., Starukhina, L., Hoffmann, H., & Arnold, G. 1999, Icarus, 137, 235
[5] Thirouin A., Ortiz J., Dufard R. et al. 2010, A&A, 522, A93
[6] Shchuko O.B., Shchuko S.D., Kartashov D.V., and Orosei R. 2014, PSS, 104,147

EPSC Abstracts
Vol. 10, EPSC2015-230, 2015
European Planetary Science Congress 2015

Chiron, another Centaur with ring material

J. L. Ortiz (1), R. Duffard (1), N. Pinilla-Alonso (2), A. Alvarez-Candal (3), P. Santos-Sanz (1), N. Morales (1), E. Fernández-Valenzuela (1), J. Licandro (4,5), A. Campo-Bagatin (6), A. Thirouin (7)

(1) Instituto de Astrofísica de Andalucía-CSIC, Granada, Spain, (2) Department of Earth and Planetary Sciences, University of Tennessee, Knoxville, 37996 TN, USA, (3) Observatório Nacional, Rua General José Cristino 77, 20921-400 Rio de Janeiro, Brazil, (4) Instituto de Astrofísica de Canarias, c/Vía Lactea s/n, 38200 La Laguna, Tenerife, Spain, (5) Departamento de Astrofísica, Universidad de La Laguna (ULL), 38205 La Laguna, Tenerife, Spain, (6) Departamento de Física, Ingeniería de Sistemas y Teoría de la Señal, Universidad de Alicante, Carretera San Vicente del Raspeig s/n, 03690 San Vicente del Raspeig, Alicante, Spain, (7) Lowell Observatory, 1400 W Mars Hill Rd, Flagstaff, 86001 Arizona, USA (ortiz@iaa.es)

Abstract

Chariklo is known to possess an exotic ring system and we show indications from several distinct data sets that Chiron also has a ring system with similar features to that of Chariklo, although its case is somewhat more complex because Chariklo has never shown cometary-like activity, whereas Chiron has.

1. Introduction

After the finding (through a stellar occultation in 2013) that a body of non-planetary dimensions named Chariklo has a dense ring system of two narrow and dense rings separated by a gap [1], we wondered whether other solar system bodies similar to Chariklo could have rings. It turns out that Chiron, another Centaur similar to Chariklo in size also shows clear indications that it could have a ring system. As recently reported [2] there are observations of past stellar occultations caused by Chiron in which there are sudden and brief brightness decreases nearly identical to those caused by the rings of Chariklo, but they had not been attributed to rings. The sudden brightness drops had been interpreted as due to a dust jet [3,4,5], probably because the occultations were not recorded from several observatories, in contrast to the Chariklo occultation in 2013, which was widely observed.

2. Reanalysis of past occultations

The occultation by Chiron in 2011 is the one that more closely resembles that of Chariklo, but only two chords were obtained [5]. Using the times when the sudden brightness drops occurred to plot the events in the plane of the sky, and putting the additional constraint that the rings ellipse and the ellipse that represents the projected shape of Chiron are concentric, the rings orientation can be derived [2]. The two possible orientations are consistent with earlier occultation events although the rings material is not homogeneously distributed and seems to be absent at certain longitudes.

3. Another indication: Long term brightness changes

Chiron's brightness variations along four decades can be explained, overall, by the presence of a reflecting ring system that contributes nothing to Chiron's brightness when the system is edge-on with respect to the Earth observers, while currently a considerable fraction of Chiron's brightness comes from the rings. The orientation of the ring system that can explain the historical time series is coincident with the orientation derived from the reanalysis of the stellar occultations.

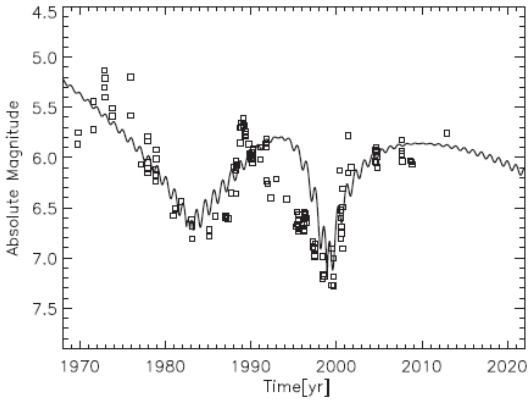

Figure 1. Solid line: Model to explain Chiron's overall absolute magnitude in V band whose key feature is the incorporation of a ring system [2]. The square symbols are the observations.

4. Another indication: Water ice spectroscopic features

The variable water ice spectroscopic feature in Chiron, which depends on the epoch when it was observed [6], can be explained if Chiron's water ice is in the rings. This can even explain the total disappearance of the water ice feature in 2001 reported in [7], because in 2001 the ring system was close to the edge-on position. All this makes sense and is exactly the same as observed for Chariklo, whose water ice is in the rings [8]. We know that Saturn's rings are rich in water ice while the cometary surfaces, the closest analog to Centaur surfaces, are devoid of spectroscopic water ice features. Hence, it appears natural that the water ice feature comes from the rings.

5. Another indication: rotational lightcurve amplitude change

There is yet more evidence for a ring system. The amplitude of the rotationally-induced oscillation of Chiron's brightness has been changing over the years. A simple model that uses the rings system orientation derived above and that incorporates the brightness of the rings, can explain the observed changes (Fig. 2).

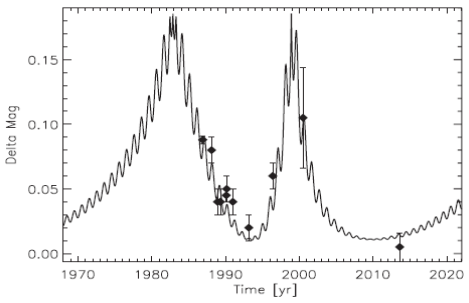

Figure 2. In continuous line we show a model of the change in the amplitude of Chiron's rotational brightness oscillation. This model incorporates the orientation of the ring determined from the occultation. The filled diamonds represent the observations. As can be seen, the fit is remarkably good.

6. More indications

The albedo of the ring system used in the brightness and spectroscopy models is identical. And the ring systems in Chariklo and Chiron have very similar optical depths and sizes, with even a gap of similar size in between. All these coincidences point to a similar origin. Besides, the alternative explanation of a jet or shell for Chiron's brightness drops does not hold because the jet or shell would have to have exotic properties. On the other hand, there was no activity that could sustain a jet or shell at the epochs when the occultations were recorded.

7. Discussion

The origin of the rings in these bodies is not yet clear. There have been different scenarios proposed and their implications for our understanding of the solar system are important and diverse. Some of these are discussed in some detail in [2], where several speculations and ideas have been presented.

References

[1] Braga-Ribas et al. Nature 508, 72 (2014)
[2] Ortiz et al. Astron. Astrophys . 576, A18 (2015)
[3] Elliot et al. Nature 373, 46 (1995)
[4] Bus et al. Icarus 123, 478(1996)
[5] Ruprecht et al. DPS meeting 45, 414.07 (2013)
[6] Groussin et al. Astron. Astrophys. 413, 1163 (2004)
[7] Romon-Martin et al. Astron. Astrophys 400, 369 (2003)
[8] Duffard et al. Astron. Astrophys. 568, A79 (2014)

EPSC Abstracts
Vol. 10, EPSC2015-251-1, 2015
European Planetary Science Congress 2015

Pluto's atmosphere structure from ground-based stellar occultations

E. Meza (1) B. Sicardy (1), E. Lellouch (1), A. Dias-Oliveira (2), D. Bérard (1), M. Assafin (3), F. Braga-Ribas (4), J. I. B. Camargo (2), G. Benedetti-Rossi (2), R. Vieira Martins (2,3), J.H. Girard (5), J. Pollock (6), E. Jehin (7), J.L. Ortiz (8), R. Duffard (8), D. E. Reichart (9), A. P. LaCluyze (9), J. B. Haislip (9), K. M. Ivarsen (9), W. Beisker (10), D. Herald (11), D. Gault (11), J. Talbot (11), H.-J. Bode (10), T. Barry (12), Broughton, J. (12), Hanna, W. (12), Bradshaw, J. (11), Kerr, S. (12,13), Pavlov, H. (14)
(1) LESIA, Observatoire de Paris, CNRS UMR 8109, Université Pierre et Marie Curie, Université Paris- Diderot, 5 place Jules Janssen, F-92195 Meudon Cedex, France (erick.meza@obspm.fr, tel: +33-(0)1-45077492). (2) Observatório Nacional/MCTI, Rua General José Cristino 77, CEP 20921-400 Rio de Janeiro, RJ, Brazil. (3) Observatório do Valongo/UFRJ, Ladeira Pedro Antonio 43, CEP 20.080-090 Rio de Janeiro, RJ, Brazil. (4) Federal University of Technology - Paraná (UTFPR/DAFIS), Curitiba, PR, Brazil. (5) European Southern Observatory, Alonso de Córdova 3107,Vitacura, Casilla 19001 Santiago 19, Chile. (6) Physics and Astronomy Department, Appalachian State University, Boone, North Carolina 28608, USA. (7) Institut d'Astrophysique de l'Université de Liège, Alleé du 6 Août 17, B-4000 Liège, Belgium. (8) Instituto de Astrofísica de Andalucía, CSIC, Apt 3004, 18080, Granada, Spain. (9) Department of Physics and Astronomy, University of North Carolina - Chapel Hill, North Carolina 27599, USA. (10) International Occultation Timing Association - European Section, Germany. (11) International Occultation Timing Association, worldwide, USA. (12) Royal Astronomical Association of New Zealand RASNZ, Occultation Section, New Zealand. (13) Astronomical Association of Queensland, Australia. (14) Tangra Observatory, 9 Chad Place, St. Clair, NSW, Australia.

Abstract

Stellar occultations are a unique tool to study Pluto's atmosphere at pressure levels ranging from 10 μbar to about 0.1 μbar. Within those limits, they provide density, pressure and temperature profiles of the atmosphere. Here we report results obtained during campaigns that we organized to observe Pluto stellar occultations on 18 July 2012 and 04 May 2013. We will also report results from campaigns in 2015 (if successful), in particular the 29 june 2015 event in Australia and New Zealand, and the 26 July 2015 occultation in South America.

1. Introduction

The 18 July 2012 and 04 May 2013 stellar occultations by Pluto were among the best ever observed in terms of signal-to-noise ratios (SNR's) obtained and latitudinal coverage of the dwarf planet. The 2012 event was recorded from five different sites in South America, while the 2013 occultation was observed from six different sites, also in South America. Both occultations were recorded at the 8.2-m Very Large Telescope (VLT) of the European Southern Observatory using the NACO camera in H band. That instrument provided among the best SNR light-curves ever obtained during Pluto stellar occultations.

2. Results

Fig. 1 shows the temperature profiles retrieved from the inversions of the light-curves obtained in 2012 and 2013. In this diagram, the temperature T is plotted against r, the distance to Pluto's center. The profiles are obtained under the assumptions that Pluto's atmosphere is spherically symmetric and transparent (no hazes), see [1] for details.

Several features are noteworthy: (1) a strong positive temperature gradient at the bottom of the profiles, consistent with the presence of a stratosphere that connects the surface (temperature 40-55 K) to the upper atmosphere; (2) a distinctive temperature maximum of $T \approx 110$ K near r=1,220 km; and (3) a mesosphere with a negative temperature gradient of about -0.2 K km^{-1}. Possible origins of this negative gradient will be discussed, in particular the possible cooling role of species such as CO or HCN. The negative gradient could also be an apparent effect (i.e. the atmosphere could be isothermal) caused by unmodeled processes such as a partial differentiation of molecular nitrogen and neon, or the presence of zonal winds around $r = 1,250$ km. We will show that none of those explanations satisfactorily explains the observed mesospheric trend.

The inversions also provide pressure profiles for the two events, with values of 2.16 ± 0.02 μbar and $2.30 \pm$

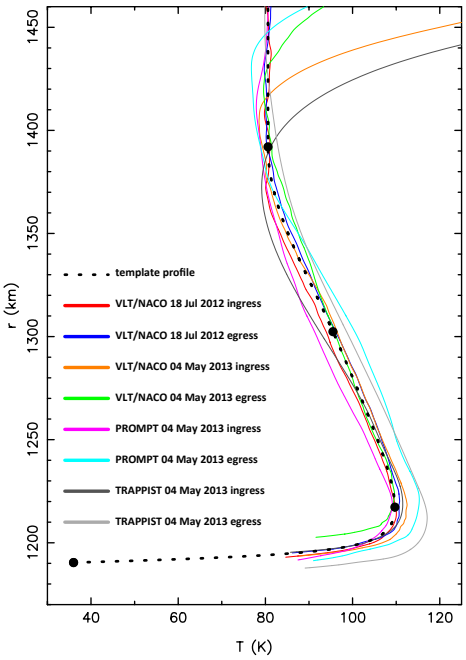

Figure 1: Pluto's atmospheric temperature profiles derived from the inversion of the light-curves obtained during the Pluto stellar occultations of 18 July 2012 and 04 May 2013. The radius r on the vertical axis is the distance to Pluto's center. The diverging behavior of the profiles observed at the top of the panel is caused by the increasing contribution of noise to the retrieved temperature profiles. The dotted line is a smooth atmospheric model that best fits our observed profiles.

0.01 μbar at $r = 1,275$ km for the 18 July 2012 and 04 may 2013 events, respectively. This is a small (6%) but significant (6-σ level) increase of pressure between the two dates, confirming with better accuracy the results of [2].

3. Future campaigns

At the moment of submission, we are planning campaigns to observe the 29 June 2015 Pluto occultation in Australia and New Zealand, as well as the 26 July 2015 event in South America.

The goal is to monitor Pluto's atmosphere two years after the events described above, and at the moment of the NASA *New Horizons* Pluto flyby of 14 July 2015. Preliminary results will be presented if good quality data are obtained during those campaigns.

Acknowledgements

The authors acknowledge support from the French ANR grant 11-IS56-0002 'Beyond Neptune II' (Programme Blanc International).

Based on observations made at ESO-Paranal with runs 089.C-0314(C) and 290.C-5084(B), using the VLT "Yepun" NACO camera.

References

[1] Dias-Oliveira, A. *et al.*: Pluto's atmosphere from 18 july 2012 and 04 may 2013 stellar occultations, in preparation, 2015.

[2] Olkin, C.B. *et al.*: Evidence that Pluto's atmosphere does not collapse from occultations including the 2013 May 04 event, Icarus, Vol. 246, pp. 220-225, 2015.

EPSC Abstracts
Vol. 10, EPSC2015-272, 2015
European Planetary Science Congress 2015

The Formation of Neptune Trojans under a Planetary Instability Migration Model

Rodney Gomes
Observatório Nacional, Rio de Janeiro, Brazil (rodney@on.br)

Abstract

A numerical integration of the equations of motion of the four giant planets and a disk of $\sim 3 \times 10^4$ planetesimals is done. The planetesimals have mass to perturb the planets but not themselves. In this integration, the planets experience a phase of close encounters (Nice Model). During the integration some planetesimals are trapped into the 1:1 mean motion resonance with Neptune, but all escape until the end of the integration. I do five cloned integrations using the same migration rates of the planets as determined by the original integration, and also including 200 clones of all temporary trapped planetesimals as Neptune Trojans. In the end of this new integration some planetesimals are still in the 1:1 mean motion resonance with Neptune. From the model I estimate the mass of the Neptune Trojans at around $3 \times 10^{-4} M_\oplus$ and inclinations up to $50°$.

1. Introduction

A peculiar feature of Neptune Trojan orbits is their wide range of inclination distribution [2]. Also, the total number of these 1:1 resonators is estimated at around 150 with $H_r \leq 10.0$ [1]. I investigate the process of production of Neptune Trojans in a model of planetary migration with close encounters with the planets (Nice model [3]). Although considering around 3×10^4 particles in the original integration, no particle survives to the end of the integration as Neptune Trojan, although many of them are temporarily trapped. This is in fact expected since as the planetesimals disk's mass is estimated at $35 M_\oplus$, each particle in the simulated disk carries around $10^{-3} M_\oplus$. This is the estimated mass of the cold Kuiper belt [4], which is likely at least one order of magnitude larger than the Neptune Trojans mass. Thus I redo the original integration five times using only cloned particles from the trapped Trojans, as explained in the next Section.

2. The Numerical integrations

I mimic five times the original integration, keeping the same migration rate of the planets but changing the initial conditions so that the planets stop as close as possible to their present distance from the Sun. During each of these new integrations I place 200 clones of each temporarily trapped Trojan from the original integration. Since in the replayed integrations the planets have different orbital elements from the original ones (only the migration rate is maintained), the clones are produced with a normalized semi-major axis with respect to the corresponding Neptune from the new integrations. Eccentricities and inclinations are the same as the original ones, and the other angles are the same relative to Neptune's mean longitude. Clones are introduced at about the mean time of evolution of the Neptune Trojans in the original integration. Temporary Neptune Trojan captures in the original integration will be considered for cloning and introducing in the five test integrations whenever the particle is kept as Neptune Trojan continually for at least 10 My. In the end of each of the five integrations, I check the surviving Trojans and analyze their orbital distribution and the total number of objects left as Neptune Trojans, what allows the estimation of their mass.

3. Results

Figure 1 shows the cumulative inclination distribution considering all five integrations. We notice that most of the inclinations are in the range $10°$ to $30°$ with a few below $10°$ and above $30°$. The highest inclination is $51.2°$ and the lowest one $2.4°$. These numbers are well in accord with estimated distributions of Neptune Trojans [2]. Also the libration widths distribution looks compatible with an estimated real distribution [2]. The total mass of Neptune Trojans estimated from the five integrations range from 1.5×10^{-4} to $4.5 \times 10^{-4} M_\oplus$, which seems a little too large. I noticed however that the number of Trojans in the end of the integration is quite sensible to the mean motion ra-

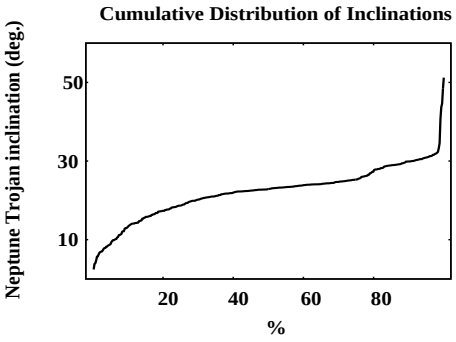

Figure 1: Cumulative Distribution of Neptune Trojans inclinations as determined by the five cloned integrations.

tio between Neptune and Uranus. When it approaches 2 the number of Trojans drops drastically. The original integration in fact suggests that although Neptune and Uranus migrated divergently most of the time, during some lapses of time the migration turned to convergent. This could even happen near the end of the integration, suggesting that Uranus and Neptune may have been a little closer to their 1:2 mean motion commensurability during the last $\sim 1Gy$.

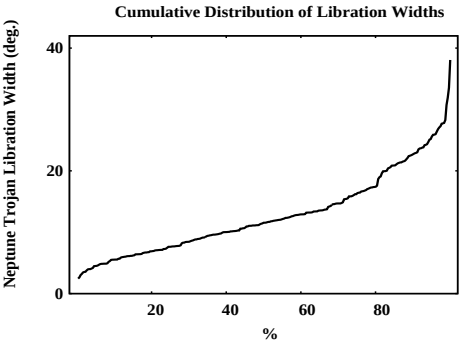

Figure 2: Cumulative Distribution of Neptune Trojans libration widths as determined by the five cloned integrations.

4. Summary and Conclusions

Numerical integrations of the equations of motion of the four giant planets and a disk of planetesimals in a case where the planets experience close approaches show temporary trappings of planetesimals into the 1:1 resonance with Neptune. These Trojans however fail to survive until the end of the integration. I run five other cloned runs from the original one, keeping the same migration rates of the planets and cloning the Trojans 200 times. Other particles are not considered in these synthetic integrations. In the end of the integrations some Neptune Trojans survive. The distribution of inclinations and libration widths are well compatible with recent results of estimation of these orbital elements from the observations [2]. I can also estimate a mass distribution for the Neptune Trojans between 1.5×10^{-4} to $4.5 \times 10^{-4} M_{\oplus}$, which is of the order of magnitude of the cold Kuiper belt mass [4]. On the other hand, Neptune Trojans population seems to be much less numerous than Kuiper Belt populations [1]. I suggest that Neptune and Uranus were a little closer to their 1:2 commensurability in the past, what is suggested by some Nice model numerical integration. This may have destabilized several Trojans producing a smaller total mass in the end. These results also reinforce the idea that the original planetesimals disk was pre-heated prior to (or heated by) Neptune's migration [2].

References

[1] Alexandersen, M., Gladman, B., Kavelaars, J., Jwyn, S., and Shankman, C., and Petit, J.-M.: A carefully characterised and tracked Trans-Neptunian survey, the size-distribution of the Plutinos and the number of Neptunian Trojans, eprint arXiv:1411.7953, 2015.

[2] Parker, A.: The intrinsic Neptune Trojan orbit distribution: Implications for the primordial disk and planet migration, Icarus 247, 112–125, 2015.

[3] Tsiganis, K., Gomes, R., Morbidelli, A., and Levison, H.: Origin of the orbital architecture of the giant planets of the Solar System, Nature 435, 459-461, 2005.

[4] Fraser, W., Brown, M., Morbidelli, A., Parker, A., and Batygin, K.: The Absolute Magnitude Distribution of Kuiper Belt Objects, The Astrophysical Journal 782: 100, 2014.

EPSC Abstracts
Vol. 10, EPSC2015-309, 2015
European Planetary Science Congress 2015

JWST observations of stellar occultations by transneptunian objects and centaurs

P. Santos-Sanz (1), R. G. French (2), Z-Y. Lin (3), N. Pinilla-Alonso (4), J. Stansberry (5), Z-W. Zhang (6), J.L. Ortiz (1) and R. Duffard (1)

(1) Instituto de Astrofísica de Andalucía-CSIC, Granada, Spain, (2) Department of Astronomy, Wellesley College, Wellesley, MA 02481, USA, (3) Institute of Astronomy, National Central University, Jhongli City, Taoyuan County 32001, Taiwan, (4) Department of Earth and Planetary Sciences, University of Tennessee, Knoxville, 37996 TN, USA, (5) Space Telescope Science Institute, 3700 San Martin Drive, Baltimore, MD 21218, USA, (6) Institute of Astronomy and Astrophysics, Academia Sinica, P.O. Box 23-141, Taipei 10617, Taiwan (psantos@iaa.es)

Abstract

We investigate the capabilities provided by the James Webb Space Telescope (JWST) for the study of transneptunian objects (TNOs) and centaurs by means of the stellar occultation technique [1]. The strengths and weaknesses of this technique are evaluated in light of JWST's unique capabilities. We identify several possible JWST occultation events by TNOs and centaurs from 2018 to 2023, and evaluate their potential scientific value [1]. We also explore the possibility of serendipitous stellar occultations by very small TNOs as a by-product of other JWST observing programs.

1. Introduction

The observation of stellar occultations by solar system objects is a very powerful technique. Obtaining the timing of disappearance / reappearance of a star behind the object's limb from different locations, allows to obtain different chord lengths and to determine a very accurate size ($\sigma \sim 0.1\%$) and shape for these bodies. The detection of atmospheres, satellites, and the discovery/characterization of ring systems (as those detected around the centaurs Chariklo [2] and Chiron [3]) are other relevant products that we can obtain from stellar occultations.

Stellar occultations by Pluto were the first occultations by a TNO predicted and detected, and illustrate very well the power of this technique [4], [5]. Apart from Pluto, the observation of stellar occultations by TNOs is a relatively new field: only ~ 17 occultations by 9 TNOs have been recorded so far from ground-based telescopes (*e.g.* [6], [7], [8]), heightening the importance of identifying opportunities with other facilities, like space-based telescopes such as HST and JWST.

Stellar occultations are also a powerful tool to explore outer solar system small objects, whose sky-plane density is large enough to generate serendipitous stellar occultations. From these serendipitous occultations we can detect tiny objects invisible by direct imaging (*e.g.* [9]).

Both kinds of stellar occultations (predictable and serendipitous) require high-SNR and high time resolution observations of faint target stars which can be provided by JWST.

2. Predictable stellar occultations

Predictable stellar occultations are those that can be anticipated, i.e. it is possible to estimate when the occultation will occur, and where it will be visible. The main difficulty of this technique lies in the prediction of the events, which are rare due to the extremely small apparent size of the TNOs/centaurs (typically ~10 mas or even smaller) and the uncertainties in the orbit determination (due to the short arc of the orbit observed). The situation has improved spectacularly over the last few years thanks to improved ephemerides and star catalogues, and it will improve even more in the next years with the GAIA catalogue.

There is an additional source of uncertainty to predict occultations visible from JWST which is the position of the observatory in its orbit around L2 point. The expected accuracy of the JWST ephemeris is currently under study, and will be an important factor

in estimating how well one can predict stellar occultations well in advance of the event.

Unfortunately, for occultations observed from JWST it is likely that only a single-chord will be obtained, since the event geometry will not provide the opportunity to observe the same occultation from ground-based (or space-based) observatories. However, even a single-chord occultations can be scientifically valuable [10]. For example, a single-chord observation could detect localized or global atmospheres at ~10 nbar level [7, 8]. With sufficiently high SNR, it could allow the retrieval of vertical profiles of atmospheric pressure and temperature. Single-chord occultations also provide the opportunity for serendipitous discovery and characterization of satellites and rings around TNOs or centaurs.

3. Serendipitous stellar occultations

Besides the predictable stellar occultations technique we can detect random stellar occultations, i.e. detect the diffraction shadow pattern in serendipitous stellar occultations by small numerous TNOs [9, 11]. These serendipitous occultations have no other competing methods, as the magnitudes of the corresponding objects, V ∼ 35 mag or fainter, are unreachable through classical ground-based –or even space-based– imaging. The method is successful if the sky density of objects is sufficient to result in a significant number of observable events.

Such occultations can reveal the vertical and radial distribution of the TNOs as far as 50 AU and beyond (kilometre-sized objects could be detected at ∼ 500 AU). Also, they provide information on the size distribution down to hectometre-sized and smaller objects, which is a key constraint to characterize the collisional history in the transneptunian belt.

The Fine Guidance Sensor (FGS) is a key component of the JWST Attitude Control System (ACS), and could be used as a unique instrument for high-speed photometry as well because it will image guide stars at a cadence of 16 Hz. We propose using FGS to detect serendipitous stellar occultations by TNOs, as a sub-product of other observing programs.

References

[1] Santos-Sanz, P., French, R. G., Lin, Z-Y., et al. 2015, submitted to PASP.

[2] Braga-Ribas, F., Sicardy, B., Ortiz, J. L., et al. 2014, Nature, 508, 72.

[3] Ortiz, J.L., Duffard, R., Pinilla-Alonso, N., et al. 2015, A&A, 576, A18.

[4] Hubbard, W.B.; Hunten, D.M.; Dieters, S.W., Hill, K.M., & Watson, R.D. 1988, Nature, 336, 452.

[5] Elliot, J.L.; & Young, L.A. 1992, Astronomical Journal, 103, 991.

[6] Elliot, J.L., Person, M.J., Zuluaga, C.A., et al. 2010, Nature, 465, 897.

[7] Sicardy, B., Ortiz, J. L., Assafin, M., et al. 2011, Nature, 478, 493.

[8] Ortiz, J. L., Sicardy, B., Braga-Ribas, F., et al., 2012, Nature, 491, 566.

[9] Roques, F., Georgevits, G., & Doressoundiram, A. 2008, The Solar System Beyond Neptune, 545-556.

[10] Alvarez-Candal, A., Ortiz, J. L., Morales, N., et al., 2014, A&A, 571, A48.

[11] Roques, F., Boissel, Y., Doressoundiram, A., Sicardy, B., & Widemann, T. 2009, EM&P, 105, 201

EPSC Abstracts
Vol. 10, EPSC2015-365, 2015
European Planetary Science Congress 2015

The November 14th, 2014 Stellar Occultation by the TNO 2007UK126

G. Benedetti-Rossi (1), F. Braga-Ribas (1,2), B. Sicardy (3), M. Buie (4), R. Vieira-Martins (1), J. I. B. Camargo (1), M. Assafin (5), J. L. Ortiz (6) and J. Desmars (7)
(1) Observatório Nacional (ON/MCTI), Rio de Janeiro, Brazil (gustavorossi@on.br / Fax: +55-21-25897463, (2) Universidade Tecnológica Federal do Paraná (UTFPR), Curitiba, Brazil, (3) LESIA, Observatoire de Paris, CNRS UMR 8109, Université Pierre et Marie Curie, Université Paris-Diderot, Meudon, France, (4) South Western Research Intitute, SwRI, Boulder, USA, (5) Observatório do Valongo, OV/UFRJ, Rio de Janeiro – Brazil, (6) Instituto de Astrofísica de Andalucía, CSIC, Granada, Spain, (7) IMCCE, Observatoire de Paris, CNRS UMR 8028, Paris, France

Abstract

We report the observation of a multi-chord stellar occultation by the transneptunian object (TNO) 2007 UK126. The event was observed by the RECON network and other collaborators on November 14, 2014 UT from seven sites in the United States. With a diameter of about 600 km and orbiting at about 43.5 AU, this recently discovered object is listed as highly likely a dwarf planet. Some of its physical parameters could be derived from this occultation.

1. Introduction

Stellar occultation is one of the best methods used to acquire precise information on the Trans-Neptunian Objects (TNOs) and Centaurs. Km-sizes [1,9] and nano-bar atmosphere [10,2,11] can be obtained with this method. Shape, albedo[2], density, surface properties [7] presence of rings [1] or other structures such as jets, and other physical parameters can be also derived [9].

Those physical parameters of the TNOs provide important information on their formation and evolution. Orbiting at more than 30 Astronomical Units (AU) from the Sun, those objects are less affected by interplanetary radiation and have low rate of mutual collision. For this reason, they can be considered as remnants, relatively unaltered, of the solar system formation [5].

Besides that, information about the TNOs are of great relevance when one tries to establish a more general formation scenario for planetary systems, also needed for the most recent extra-solar systems discovered. The problem is that TNOs have a diameter smaller than 2,300 km (Eris, one of the biggest has 2326 km [10]) and when seen from Earth they appear smaller than 50 mili-arcseconds in the sky and not very bright, so that it is extremely hard to resolve such objects with the actual imaging systems.

One of the biggest known TNO is called 2007 UK126 [8]. With a diameter of about 600 km and orbiting at about 43.5 AU, this recently discovered object is listed as highly likely a dwarf planet [3] and it occulted [5] a star in November 14, 2014. Its shadow crossed USA where the RECON [4] network and other collaborators obtained 7 occultation chords from which we could obtain some of its physical parameters.

Observations were made in 4 different locations from the RECON: Gardnerville, Tonopah, Yerington, and Carson City (2 chords); and also two more chords were obtained in San Pedro Martir (negative) and by the IOTA team. Figure 1 shows the prediction map for the event.

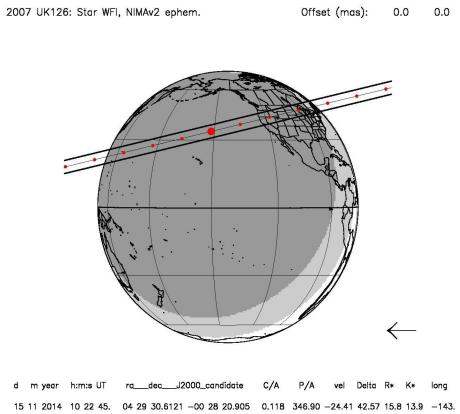

Figure 1: Prediction map for the occultation of a MagR= 15.8 star by the TNO 2007 UK126. The

bigger red dot represents the closest approach (10:22:45 UT) and other dots are one minute spaced (crescent to the left). Map generated using the NIMA ephemerides [6].

2. Results

The positive detections yields seven occultation chords. The ongoing reduction will allow to determine size and shape of the object. Also, one negative detection is important to determine limits on its values. Considering only the longest observed chord, we can calculate the lower limit to the semi-major axis of 2007 UK126 as R= 337±21 km.

From the determined size and shape we will derive its density, considering that is in hydrostatic equilibrium, and put a lower limit on the presence of atmosphere. By using current estimations for its magnitude, we can also infer a geometric albedo for the body.

3. Summary and Conclusions

From the stellar occultation data of November 14, 2014, (ongoing) it will possible to obtain some important physical characteristics for the TNO 2007 UK126 such as size, shape, density and albedo.

Furthermore, the observation demonstrates that occultations of faint stars (here ~15.8) can be detected through modest instruments and depends on a international collaboration. This is made possible as sensitive cameras and better astrometric predictions are available and continues a new era of discoveries because faint stars are far more numerous than bright ones. This allows us to determine the size of remote (e.g. trans-neptunian) objects at kilometric accuracy with associated accurate values for their albedo and density.

Acknowledgements

We thank CAPES for the financial support, all people involved on the RECON who participated on this campaign.

References

[1] Braga-Ribas, F., Sicardy, B., Ortiz, J. L. et al.: A ring system detected around the Centaur (10199) Chariklo, Nature, Vol. 508, pp. 72, 2014.

[2] Braga-Ribas, F., Sicardy, B., Ortiz, J. L. et al.: The Size, Shape, Albedo, Density, and Atmospheric Limit of Transneptunian Object (50000) Quaoar from Multi-chord Stellar Occultations, ApJ, Vol. 773, pp. 26, 2013

[3] Brown, M., California institute of Technology, http://web.gps.caltech.edu/~mbrown/dps.html

[4] Buie, M. Keller, J. M.: TNO Occultations with RECON, AAS DPS Meeting #45, #511.08, 2013

[5] Camargo, J. I. B. et al.: Candidate stellar occultations by Centaurs and trans-Neptunian objects up to 2014, A&A, Vol. 561 pp. A37, 2014

[6] Desmars, J. et al.:Improvement of TNO's ephemeris in the context of stellar occultations, Revista Mexicana de Astronomia y Astrofisica Conference Series, Vol. 44, pp. 130-131, 2014

[7] Elliot, J. L., Person, M. J., Zuluaga, C. A., et al.: Size and albedo of Kuiper belt object 55636 from a stellar occultation, Nature, Vol. 465, pp. 897-900

[8] IAU Minor Planet Center, http://www.minorplanetcenter.net/iau/lists/t_tnos.html

[9] Ortiz, J. L., Sicardy, B., Braga-Ribas, F.: Albedo and atmospheric constraints of dwarf planet Makemake from a stellar occultation, Nature, Vol. 491, pp. 566-569, 2012

[10] Sicardy, B., Ortiz, J. L., Assafin, M., et al.: A Pluto-like radius and a high albedo for the dwarf planet Eris from an occultation, Nature, Vol. 478, pp. 493-496, 2011

[11] Widemann, T., Sicardy, B., Dusser, R., et al.: Titania's radius and an upper limit on its atmosphere from the September 8, 2001 stellar occultation, Icarus, vol. 199, pp. 458-476

EPSC Abstracts
Vol. 10, EPSC2015-417, 2015
European Planetary Science Congress 2015

The Successful Search for a Post-Pluto KBO Flyby Target for New Horizons Using the Hubble Space Telescope

J. R. Spencer (1), M. W. Buie (1), A. H. Parker (1), H. A. Weaver (2), S. B. Porter (1), S. A. Stern (1), S. D. Benecchi (3), A. M. Zangari (1), A. J. Verbiscer (4), S. D. J. Gwyn (5), J-M. Petit (6), J. J. Kavelaars (5), R. Sterner (2), D. M. Borncamp (7), K. S. Noll (8), D. J. Tholen (9), M. R. Showalter (10), C. I. Fuentes (11), M. J. S. Belton (12), R. P. Binzel (13). (1) Southwest Research Institute, Colorado, USA (spencer@boulder.swri.edu), (2) Johns Hopkins U./APL, Maryland USA, (3) Planetary Science Inst., USA, (4) U. Virginia, USA, (5) Herzberg Inst. of Astrophysics, Canada, (6) Obs. De Besancon, France, (7) Space Telescope Science Inst., Maryland, USA, (8) NASA/GSFC, Maryland, USA, (9) U. Hawaii, USA, (10) SETI Inst., California, USA, (11) Northern Arizona U., USA, (12) Retired, (13) MIT, Massachusetts, USA

Abstract

After four years of ground-based searching for a Kuiper Belt object flyby target for the New Horizons (NH) spacecraft beyond Pluto, a large search with the Hubble Space Telescope in 2014 discovered two KBOs reachable by NH. The spacecraft will be diverted towards one of these objects in late 2015, after the Pluto encounter, and a close flyby in 2018 – 2019 will be proposed as part of a potential NH extended mission.

1. Introduction

The New Horizons mission [1], which will make the first flyby of the Pluto system in July 2015, has the expected longevity and fuel reserves to continue deeper into the Kuiper Belt and fly by at least one additional small Kuiper Belt object (KBO). Additional KBO flybys were recommended as a key component of the Pluto mission by the 2003 Planetary Decadal Survey [2]. The first closeup observations of typical KBOs from a flyby spacecraft are likely to revolutionize our understanding of this major component of the solar system.

New Horizons' available fuel provides a KBO targeting budget of ~130 m/sec delta-V, which provides access to a narrow cone of space within the Kuiper Belt that was predicted to contain several KBOs brighter than R magnitude 27.0 [3]. No previously-known KBOs pass through this region, so a dedicated search for suitable targets was required.

An intensive ground-based search was carried out from 2011 to 2014, using primarily the SuprimeCam camera on the Subaru telescope in Hawaii, and the Megacam camera on the Magellan telescopes in Chile. Extremely crowded background star fields (the search area is near the galactic center) limited search depth to R ~ 26.0 even in optimal seeing. The ground-based search discovered about 50 faint new KBOs. However, none is reachable by NH: the most accessible groundbased discovery would require 1.6× more fuel than the NH targeting delta-V budget.

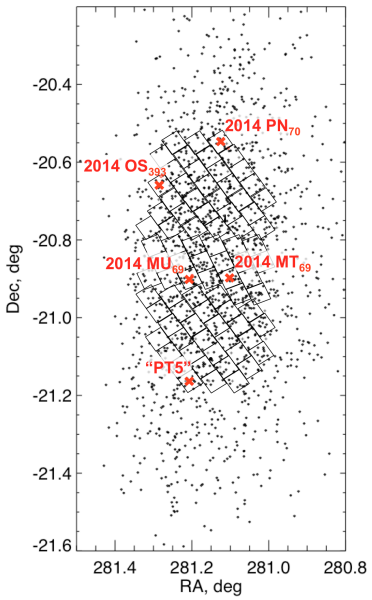

Figure 1. HST search design. Each square shows a WFC3 field, superposed on the expected distribution of targetable cold classical KBOs (dots). Red crosses identify the fields containing our five robust HST KBO detections. Positions are shown for July 1st 2015

2. Searching with HST

In 2014 we turned to the Hubble Space Telescope (HST) for a deeper search. HST provides unmatched sensitivity to faint objects in crowded fields due to its combination of high spatial resolution and stable imaging performance. We were granted 194 orbits of HST time in the Cycle 22 Guest Observer program in June 2014 (program GO-13633), including 40 orbits of Director's Discretionary time. We also added 6 orbits from HST KBO programs GO-13311 and GO-13663 [S. D. Benecchi, PI]. Advance planning by

STScI allowed our program to begin execution less than three days after being awarded time.

We searched an area of 0.17 deg^2, covering the locations of roughly half the potentially targetable KBOs (Fig. 1) and moving at their expected mean rate, using 83 pointings of HST's Wide Field Camera 3 (WFC3) with the very broad F350LP filter, with 2 visits per pointing to detect motion. Rapid data reduction and follow-up of promising discoveries allowed orbit refinement.

We obtained astrometric solutions with < 20 mas precision for each image using a custom star catalog based on CFHT images [4]. We then stacked images at sidereal rates to generate star background templates, and subtracted these from individual frames to remove background stars. We stacked the star-subtracted images of each search field at 20 – 80 different rates [5], corresponding to the range of possible motions for cold classical KBO orbits (the class of KBOs expected to include almost all targetable KBOs). Automated routines then identified point sources in the stacked images, and we determined the reality of these sources by visual vetting (Fig. 2). We estimate search limiting magnitude, at 50% detection efficiency, to be approximately R = 27.5, determined by the recovery of synthetic KBOs implanted in the data.

3. Search Results

We made five robust discoveries of cold classical KBOs in the HST data set (Table 1). Two of these objects, 2014 MU$_{69}$ and 2014 PN$_{70}$, are reachable by New Horizons [6]. With diameters of 25 – 55 km, depending on assumed albedo, they represent a previously unexplored class of objects, geometrically midway in size between typical comet nuclei and larger Trans-Neptunian objects like Pluto.

It is not possible for NH to fly by both objects. The choice between them, which is not straightforward (2014 MU$_{69}$ requires less fuel but 2014 PN$_{70}$ is brighter) will be made in time for a targeting burn towards the chosen object in Fall 2015, after the Pluto encounter. The KBO encounter, and distant observations of other KBOs found in the HST and ground-based searches, will be proposed to NASA as part of a New Horizons extended mission.

Because this is the widest KBO survey to this depth yet accomplished, the results have important implications for the population of small KBOs [7].

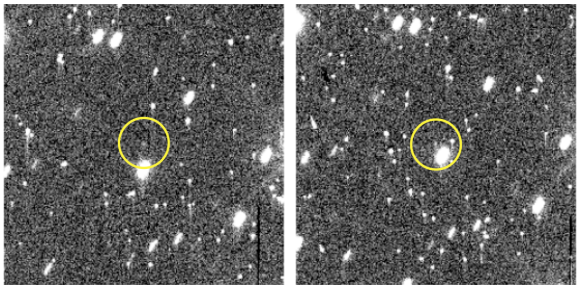

Figure 2. A small portion of two consecutive raw HST images showing 2014 MU$_{69}$ (circled), along with numerous background stars and cosmic rays. Stars are trailed because HST was tracking at the expected mean KBO motion.

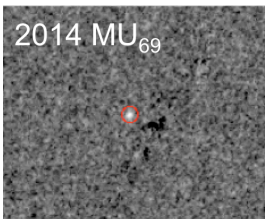

Figure 3. 2014 MU$_{69}$ (circled) after processing to combine images and remove background stars and cosmic rays

Table 1: The five robust KBO discoveries made in our HST search program. The two objects that require less than our 130 m/sec delta-V budget, and which are thus expected to be reachable by New Horizons, are highlighted in green.

Name	R Mag-nitude	Estimated Diameter		Target-ing Delta-V, m/sec	First Seen, 2014	Arc Length, Days	Encounter Date
		Albedo = 0.15	Albedo = 0.04				
2014 MU69	26.8	25 km	45 km	59	26-Jun	118	12/30/2018
2014 OS393	26.3	30 km	55 km	181	30-Jul	83	
2014 PN70	26.4	30 km	55 km	118	6-Aug	76	3/16/2019
2014 MT69	27.4			n/a	24-Jun	40	
"PT5"	26.9			n/a	8-Jul	< 1	

References

[1] Stern, S. A. (2008) *Space Sci. Rev.* **140**, 3–21.

[2] Space Studies Board, National Research Council (2003) *New Frontiers in the Solar System: An Integrated Exploration Strategy.* National Academies Press.

[3] Spencer J. R. et al. (2003) *Earth, Moon, Planets* **92**, 483–491.

[4] S. D. J. Gwyn (2015). arXiv:1411.3344 http://arxiv.org.

[5] Parker, A. H. and J. J. Kavelaars (2010) *PASP* **122**, 549–559.

[6] Porter, S. B. et al. (2015), LPSC 2015.

[7] Parker, A. H. et al. (2015), LPSC 2015.

EPSC Abstracts
Vol. 10, EPSC2015-424, 2015
European Planetary Science Congress 2015

Search for serendipitous Oort Cloud Object occultation in X-rays

Jie-Rou Shang* (1), Chih-Yuan Liu (1), Hsiang-Kuang Chang (1), Kuan-Ting Chen (2)
(1) Institute of Astronomy, National Tsing Hua University, Hsinchu, Taiwan (* Contact:: bandyshang@gmail.com),
(2) Taipei Municipal ChengGong Senior High School, Taipei, Taiwan

Abstract

The existence of Oort cloud objects remains a hypothesis since proposed more than half a century ago. Here we report the results of search for serendipitous occultation events caused by Oort Cloud Objects (OCOs) using Rossi X-ray Timing Explorer/Proportional Counter Array (RXTE/PCA) data of Sco X-1 taken from 1996 February to 2012 January. We also investigate the dependence of detection efficiency on OCO size to better define the sensible size range of our approach.

1. Introduction

Serendipitous occultation search is an indirect way used to study small outer Solar system objects (e.g., Kuiper Belt Objects (KBOs) and OCOs) by extracting and analyzing diffraction patterns in the occultation light curves. From the literature, there are already several possible detections or upper-limits reported in both optical and X-ray bands by using this method for the search of small KBOs.

Bedsides KBOs, this method also has the potential to extend the search to a distance as far away as the Oort cloud region (beyond a few thousands AU). As the distance is larger, a point source may not be a good approximation of the background source since the projected emitting area could be comparable or larger than a Fresnel scale. The X-ray emitting region in Sco X-1, based on different models, varies from about 50 km to 50,000 km, the latter of which translates to about 1 Fresnel scale at 4000 AU for X-rays at 4 keV, and about 3 Fresnel scales at 36000 AU. We consider all these factors in the investigation of detection efficiencies of our approach. Figure 1 shows some computed diffraction patterns.

We are analyzing Sco X-1 data taken by RXTE/PCA from 1996 February to 2011 October, in total about 1 Msec, to find dip events at time scales of a few tens milliseconds. We expect to report in the meeting our findings.

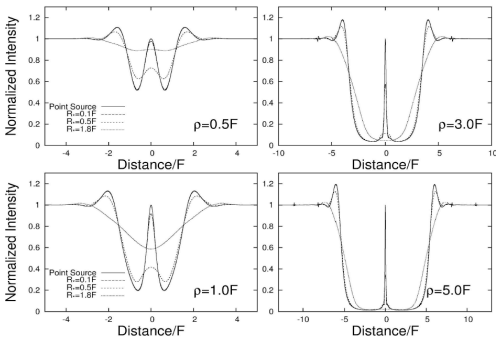

Figure 1: Diffraction intensity profiles for different occulting object and background source sizes with a given background source emission spectrum. Different panels are for different occulting object sizes. Each curve in a panel is for different background source sizes. “F” stands for the Fresnel scale.

References

[1] Hsiang-Kuang Chang; Chih-Yuan Liu; Kuan-Ting Chen: Search for serendipitous trans-Neptunian object occultation in X-rays, 2013, MNRAS 429, 1626–1632

[2] Roques, F.; Moncuquet, M.; Sicardy, B.: Stellar occultations by small bodies - Diffraction effects, 1987, AJ, 93, 1549

EPSC Abstracts
Vol. 10, EPSC2015-433, 2015
European Planetary Science Congress 2015

A Magnitude Limited Survey of the Rotational Properties of Kuiper Belt Objects

R. Kokotanekova (1,2), P. Lacerda (1), C. Snodgrass (2), M. Lockhart (3), S. Lorek (1), N. Peixinho (4), A. Thirouin (5), B. Carry (6), B. Davidsson (3), S. Fornasier (6), M. Wyatt (7), O. Hainaut (8)
(1) Max Planck Institut für Sonnensystemforschung, Göttingen, Germany (2) The Open University, Milton Keynes, UK (3) Uppsala University, Department of Physics and Astronomy, Sweden (4) Unidad de Astronomia, Facultad de Ciencias Basicas, Universidad de Antofagasta, Chile (5) Lowell Observatory, Flagstaff, Arizona, USA (6) Observatoire de Paris, Site de Meudon, France (7) Institute of Astronomy, University of Cambridge, UK (8) ESO Headquarters Garching, ESO, Germany; (kokotanekova@mps.mpg.de)

Abstract

We will present the first results from a magnitude-limited survey of over 60 Kuiper belt objects (KBOs) observed within a Large Program at the 3.6-m ESO New Technology Telescope (NTT). The multi-band observations are used to obtain lightcurves for targets from all KBO dynamical classes. We are aiming to derive the individual targets' physical and rotational characteristics as well as to use the bulk properties of the different KBO populations as sources of information for their formation mechanisms and collisional history.

1. Introduction

After the discovery of the Kuiper belt [1], more than 1700 objects have been identified and classified into dynamical classes (Resonant KBOs, Hot and Cold Classical KBOs, Scattered Disc Objects and Centaurs) according to their orbital characteristics.

Despite the substantial progress in KBO studies from the past two decades, many questions remain open (e.g. the position at the time of formation; the accretion mechanisms which formed them; the sequence of gravitational interactions which lead to their migrations and the collisional interactions during the different evolutionary stages).

These questions can be addressed by studying the spin properties of the different KBO classes. Ligthcurves with sufficient S/N can be used to derive the object's lightcurve period and peak-to-peak range, Δm, which can constrain the KBOs spin state and shape. Lightcurves are therefore powerful tools in comparing different populations [2, 3] and in the detailed study of individual objects [4, 5, 6].

Previous lightcurve observations have been reported for roughly 100 KBOs [7, 8, 9]. The majority of them have been obtained with smaller 1-m or 2-m class telescopes and do not have rotation period solutions, nor useful upper limits to the variability. Furthermore, the available sample of known rotation properties may be biased towards elliptical KBOs [10] as authors tend to report lightcurve detections, while publications of cases with no detected variability are less frequent.

2. Program Description

In order to enable studies of the statistical properties of the different KBO dynamical classes, as well as to characterize the individual objects, we are performing a magnitude-limited study using the 3.6-m ESO NTT at La Silla, Chile. The program (PI P. Lacerda) was awarded 48 nights. The combination of the large aperture and the observing strategy will allow us to analyse the rotational and colour properties of $\sim$ 60 targets. The complete list of possible objects includes 85 KBOs in the main dynamical classes, which are detectable at S/N $\geq$ 50 (Table. 1). The specific targets to be observed are selected based on visibility, while priority is given to KBOs from the less-represented classes (Outer Resonants, Hot Clasicals and Cold Classicals) in order to ensure enough objects in each group. The sample includes several targets with known surface properties and 34 objects for which no rotational properties have ever been reported (Table. 2).

To avoid the possible biases of the previously available data, the observations are being analysed in a consistent way, and all results will be published, including the cases in which no periodic variations are detected.

Table 1: Distribution of the selected targets among the different dynamical classes.

Dynamical Classes	
Inner Resonants	14
Outer Resonants	9
Cold Classicals	7
Hot Classicals	7
Centaurs	20
Sacttered Objects	28
Total Sample	**85**

Table 2: Known properties of the selected targets.

Lightcurve Properties		**Surface Properties**	
No Lightcurve	34	Albedo known	55
Upper limit Δm	23	Colour known	49
Uncertain Period	21	Both (A,C) known	44
Lightcurve known	7	Haumea-type	5

3. Objectives

The use of a 4-metre class telescope allows us to obtain high S/N lightcurves for the selected objects. They are used to study both the characteristics of particular objects and the bulk properties of the different dynamical classes. In particular we are aiming to:

- Measure spin periods, and ranges of magnitude variations in order to constrain shapes and bulk densities;
- Identify contact binaries or objects with extreme shapes or spins;
- Study surface colour variations, including the presence of surface spots;
- Obtain a sample of absolute magnitudes and optical colours protected from lightcurve variability;
- Search for variations in the Δm of KBOs with known lightcurves and attempt to constrain spin obliquity;
- Use the observed Δm distribution to determine the sphericity of the different populations and try to determine the radius at which gravity dominates over material strength [11];
- Use the derived rotational properties of the different dynamical classes as constraints to their formation mechanisms and collisional history;
- Compare the derived properties of the KBO dynamical classes to those of main-belt asteroids and Trojans.

At the time when this abstract is being prepared we have observed and advanced in the analysis of 23 KBOs from all dynamic classes. At the meeting we will present the results from the first half of the survey.

References

[1] Jewitt, D. & Luu, J. 1993, Nature, 362, 730–732

[2] Sheppard, S. S. & Jewitt, D. C. 2002, Astron. J., 124, 1757–1775

[3] Lacerda, P. & Luu, J. 2006, Astron. J., 131, 2314–2326

[4] Sheppard, S. S. & Jewitt, D. 2004, Astron. J., 127, 3023–3033

[5] Lacerda, P. & Jewitt, D. C. 2007, Astron. J., 133, 1393–1408

[6] Lacerda, P. 2011, Astron. J., 142, 90

[7] Sheppard, S. S., Lacerda, P. & Ortiz, J. L. 2008, Sol. Syst. Beyond Neptune

[8] Duffard, R., Ortiz, J. L., Thirouin, A., Santos-Sanz, P. & Morales, N. 2009, Astron. Astrophys., 505, 1283–1295

[9] Benecchi, S. D. & Sheppard, S. S. 2013, Astron. J., 145, 124

[10] Thirouin, A., Ortiz, J. L., Duffard, R., et al. 2010, Astron. Astrophys., 522, A93

[11] Lineweaver, C. H. & Norman, M. 2010, eprint arXiv:1004.1091

EPSC Abstracts
Vol. 10, EPSC2015-662, 2015
European Planetary Science Congress 2015

Search for sub-kilometre trans-Neptunian objects using CoRoT asteroseismology data: Part II

Chih-Yuan Liu (1,2), Alain Doressoundiram (2), Françoise Roques (2), Hsiang-Kuang Chang (1), Jie-Rou Shang (1)
(1) Institute of Astronomy, National Tsing Hua University, Hsinchu, Taiwan, (2) LESIA, Observatoire de Paris, Meudon, France (chihyuan.liu@obspm.fr)

Abstract

We present here the analysis of about 130k star hours of CoRoT (Convection Rotation and Planetary Transits) asteroseismology observations, which is in addition to the ∼144k star hours previously analyzed by Liu et al. We will report in this meeting how many more detections of possible occultation events (POEs) by analyzing these new data sets with the serendipitous stellar occultation method.

1. Introduction

Trans-Neptunian Objects (TNOs) are the witnesses of the formation of the planets during the dynamical and collisional period of our solar system. The population characteristics of sub-kilometer TNOs may carry some important clues for the origin of the planets. However, the knowledge of them is far from enough, particularly for those smaller ones, due to very few detections. Nowadays only TNOs larger than about 25 km can be directly observed. For the TNOs not able to be directly observed, searching for serendipitous stellar occultation events is a possible method. Currently, from the literature, only 15 POEs are reported from two serendipitous surveys: 2 POEs are found by Schlichting et al. using the observations taken by the Hubble Space Telescope's Fine Guidance Sensors, and the other 13 are found in our previous work using CoRoT data (Liu et al. 2015).

2. New CoRoT AN1 Lightcurves

The new CoRoT data contains 188 level-1 asteroseismology lightcurves from 77 stars monitored within 16 observation runs. The time resolution of these lightcurves is 1-sec. The longest lightcurve is about 130.4 days and the shortest one is 1.4 days. We are now working on analyzing these data, in total about 130k star hours. The result will help us to refine our earlier estimate of TNO size distribution as shown in Figure 1.

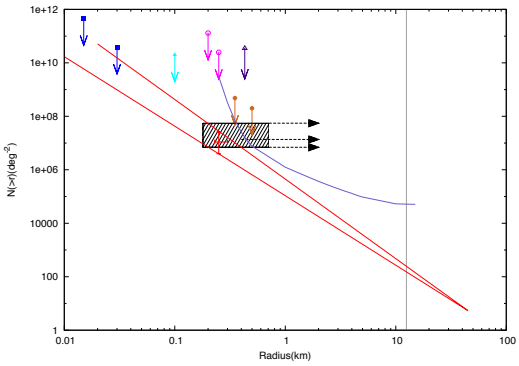

Figure 1: The size distribution derived from earlier CoRoT data (Liu et al. 2015).

References

[1] Chang H.-K., Liu C.-Y., Chen K.-T., 2013, MNRAS, 429, 1626

[2] Liu C.-Y., Doressoundiram A., Roques F., Chang H.-K., Maquet L., Auvergne, M., 2015, MNRAS, 446, 932

[3] Schlichting H. E. et al., 2012, ApJ, 761, 150

EPSC Abstracts
Vol. 10, EPSC2015-717, 2015
European Planetary Science Congress 2015

Absolute magnitudes of trans-neptunian objects

R. Duffard (1), A. Alvarez-Candal (2), N. Pinilla-Alonso (3), J.L. Ortiz (1), N. Morales (1), P. Santos-Sanz (1) and A. Thirouin (4)
(1) Instituto de Astrofísica de Andalucía, CSIC, Apt 3004, 18080, Granada, Spain. duffard@iaa.es (2) Observatório Nacional / MCTI, Rua General José Cristino 77, Rio de Janeiro, RJ, 20921-400, Brazil. (3) Department of Earth and Planetary Sciences, University of Tennessee, Knoxville, TN, 37996, United States (4) Lowell Observatory, 1400 W Mars Hill Rd, Flagsta_ff, 86001 Arizona, USA

Abstract

Accurate measurements of diameters of trans-Neptunian objects are extremely complicated to obtain. Radiomatric techniques applied to thermal measurements can provide good results, but precise absolute magnitudes are needed to constrain diameters and albedos. Our objective is to measure accurate absolute magnitudes for a sample of trans-Neptunian objects, many of which have been observed, and modelled, by the "TNOs are cool" team, one of Herschel Space Observatory key projects grantes with ~ 400 hours of observing time. We observed 56 objects in filters V and R, if possible. These data, along with data available in the literature, was used to obtain phase curves and to measure absolute magnitudes by assuming a linear trend of the phase curves and considering magnitude variability due to rotational light-curve. In total we obtained 234 new magnitudes for the 56 objects, 6 of them with no reported previous measurements. Including the data from the literature we report a total of 109 absolute magnitudes.

1. Introduction

Until recently most of the known phase curves belonged to main belt asteroids. Nevertheless, since the discovery of the trans-Neptunian objects (TNOs), some effort has been done to measure their phase curves. One critical problem for these objects is the low values of the phase angle (α) that can be reached from ground-based facilities. For comparison, a typical main belt asteroid can be observed up to 20^o or 30^o, while a typical TNO can reach only up to 3^o.

Besides providing information about surface properties, phase curves are also important because they provide the absolute magnitude, H, of an airless body. H is the reduced magnitude of an object at $\alpha = 0^o$. Moreover, H is related to the diameter of the body, D, and its albedo p. If we are considering magnitudes in V-filter, then:

$$D[km] = 1.324 \cdot 10^{(3-Hv/5)} \cdot (p_v)^{-1/2}$$

Many of the physical characteristic of the trans-Neptunian population are still hidden from us due to the limited high-quality information we can currently obtain: visible and near-infrared spectroscopy of about 100 objects [1], colours of about 300 [2] drawn from a known population of more than 1,600 objects.

2. Observations and data reduction

The data presented in this work were collected during several observing runs spanning between September 2011 and May 2014 for well over 40 nights, some of which could not be used due to bad weather conditions. The instruments and facilities used were CAFOS at the 2.2-m, CAHA2.2, and MOSCA at the 3.5-m, CAHA3.5, telescopes of the Calar Alto Observatory sited at Sierra de Los Filabres (Spain), WFC at the 2.5-m Isaac Newton Telescope, INT, sited at the Roque de los Muchachos Observatory (Spain), the direct camera at the 1.5-m telescope, OSN, of the Sierra Nevada Observatory (Spain), the SOI at the 4.1-m SOAR telescope sited at Cerro Pachón (Chile), and the direct camera at the 1-m telescope of the Observatório Astronômico do Sertão de Itaparica, OASI, Brazil.

3. Results

In total we obtained 234 new magnitudes for 56 objects, 6 of which did not have any magnitude reported before to the best of our knowledge. Alongside our own data we made an extensive,

although not complete and still on-going, search in the literature of other published V and R magnitudes. We used as our primary reference database the MBOSS 2 article by [2], but we did not take the data directly from their catalogue. Instead we carefully took the data from each referenced article to complete our list. In total we finished with over 1800 individual measurements for over 100 objects.

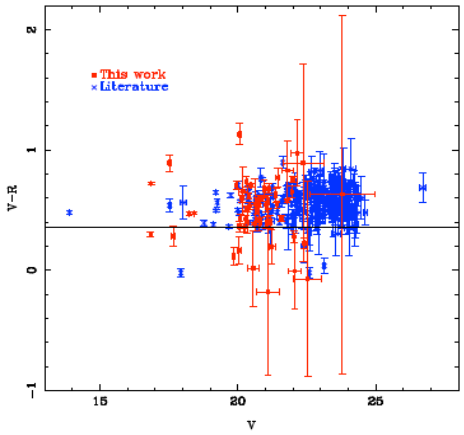

Figure 1: Color - magnitude for the objects in our database. In red are shown the objects that have at least one color measured by us, while in blue appear those whose data comes from the literature only. The $(V-R)_{\odot}$ is shown for reference as a horizontal line.

6. Summary and Conclusions

We have observed 55 objects, 6 of which with no reported magnitudes, to be the best of our knowledge, in the literature. We combined these new V and R magnitudes with an extensive bibliographic survey to compute absolute magnitudes. In total we report absolute magnitudes (H_V) for 109 objects. Some of these objects had already phase curves reported, nevertheless it is important to include new data, always keeping in mind that we are combining data from different apparitions for the same object and that surface conditions might have changed between observations.

This work represents the first release of data taken between late 2011 and early 2014 which represents a large effort of our group. It is important to mention that more observations are undergoing and that as any new work is published, and we get acquainted with, reporting new V or R magnitudes it will be included in our list, intending to have reliable H_V for all TNOs observable from 4-m class telescopes, improving at the same time the accuracy of diameters and albedos obtained via thermal data modelling.

Acknowledgements

JLO acknowledges support from the Spanish MINECO grant AYA-2011-30106-CO2-O1, from FEDER funds and from the Proyecto de Excelencia de la Junta de Andalucía, J.A. 2012-FQM1776. RD acknowledges support from the Spanish MINECO for his Ramón y Cajal contract.

References

[1] Barucci, M.A., Alvarez-Candal, A., Merlin, F., et al. 2011, Icarus, 214, 297.

[2] Hainaut, O.R., Böhnhardt, H., & Protopapa, S. 2012, A&A, 546, A115

EPSC Abstracts
Vol. 10, EPSC2015-745, 2015
European Planetary Science Congress 2015

Modeling KBOs Charon, Orcus and Salacia by means of a new equation of state for porous icy bodies

U. Malamud
Technion – Israel Institute of Technology, Haifa 32000, Israel (uri.m@tx.technion.ac.il)

D. Prialnik
Tel Aviv University, Ramat Aviv, Tel Aviv 69978, Israel (dina@planet.tau.ac.il)

Abstract

We use a one-dimensional adaptive-grid thermal evolution code to model intermediate sized Kuiper belt objects Charon, Orcus and Salacia and compare their measured bulk densities with those resulting from evolutionary calculations at the end of 4.6 Gyr. Our model assumes an initial homogeneous composition of mixed ice and rock, and follows the multiphase flow of water through the porous rocky medium, consequent differentiation and aqueous chemical alterations in the rock. Heating sources include long-lived radionuclides, serpentinization reactions, release of gravitational potential energy due to compaction, and crystallization of amorphous ice. The density profile is calculated by assuming hydrostatic equilibrium to be maintained through changes in composition, pressure and temperature. To this purpose, we construct an equation of state suitable for porous icy bodies with radii of a few hundred km, based on the best available empirical studies of ice and rock compaction, and on comparisons with rock porosities in Earth analog and Solar System silicates. We show that the observed bulk densities can be reproduced by assuming the same set of initial and physical parameters, including the same rock/ice mass ratio for all three bodies. We conclude that the mass of the object uniquely determines the evolution of porosity, and thus explains the observed differences in bulk density. The final structure of all three objects is differentiated, with an inner rocky core, and outer ice-enriched mantle. The degree of differentiation, too, is determined by the object's mass.

1. Introduction

This work [1] is an extension of a predecessor model presented by Malamud and Prialnik [2], which calculates the evolution of relatively small icy objects, having a radius of approximately 200-250 km. Here we consider the addition of physical processes that apply to much larger icy objects, with a radius of up to 600 km. In such intermediate sized icy objects the internal core pressure by self-gravity can be up to an order of magnitude larger. Therefore, we consider how these larger icy bodies react to the change in porosity as water migrates out from the core to colder regions. Maintaining hydrostatic equilibrium while various processes occur (phase changes, chemical reactions, differentiation) requires more than the parameterized EOS (Birch-Murnaghan) used in the predecessor model, which is why we devise an empirically based EOS that explicitly accounts for changes in porosity, temperature and composition. This EOS is then tested on three mid-sized KBOs, Salacia, Orcus and Charon, which can be considered a coherent sample. According to Kenyon and Bromley [3], their formation timescale is approximately 30–45 Myr, which rules out heating by short lived radionuclides (SLRs). In accretionary scenarios for growth of KBOs [4], objects are considered to form in regions that have similar physical characteristics. Thus their composition is estimated to have about the same rock/ice mass ratio. Therefore, it is reasonable to adopt the same initial composition, and the same abundance of SLRs. The main goal is to explain the present state of different objects in the Kuiper belt, starting from identical initial conditions, and using a unique set of model assumptions and parameters. We then compare the outcomes of their evolutionary computations, to measurements obtained from observations. Assuming that these selected objects were formed under similar initial conditions, we demonstrate that the differences among them (more specifically, their different bulk densities) could be explained by a single free parameter, their total mass. Note that other intermediate sized icy objects in the solar system, also have reliable bulk density

measurements, but unlike the three objects mentioned above, their evolutions may also heavily depend on initial variability in the abundance of SLRs, as well as upon their orbital, tidal and collisional histories [5], affecting the final bulk density. Collisional events are also likely to have affected several other intermediate sized KBOs [6], which are therefore not considered in this sample.

1.1 Equation of state

The EOS is we have constructed is based on the two-layer model suggested by Yasui and Arakawa [7]. The compaction curves are obtained from various empirical studies.

2. Main results

Our model and newly developed EOS can account for differentiated structures with bulk densities that are in good agreement with observed ones (Figure 1).

Figure 1: Model vs. observed bulk densities.

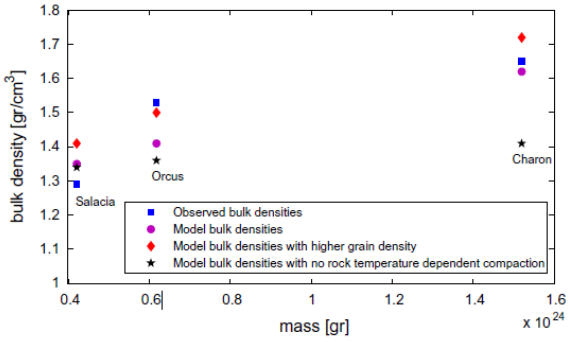

From the detailed evolution runs of Salacia, Orcus and Charon, we identify correlations between the object's mass and other physical quantities. Thus, a more massive object reaches higher temperatures, which result in a more differentiated structure. The rocky core is bigger and more compacted, while the ice-enriched mantle is smaller and has a lower rock fraction (Figure 2).

Figure 2: Final structure and composition of models, Color interpretation: *black* (pores); *white* (crystalline ice); *pink* (amorphous ice); *brown* (anhydrous rock); *olive* (aqueously altered rock)

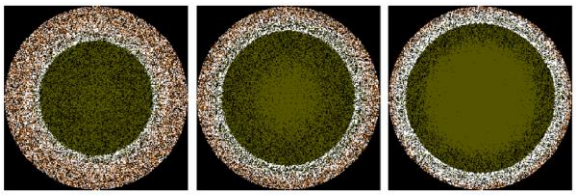

At the surface, amorphous ice can survive, but with increasing mass, its survival depth is diminished. We also find that while overall, radioactive heating is an order of magnitude more important than heating by serpentinization, in the early evolution stage their roles are reversed. Gravitational energy released due to differentiation & compaction has a marginal contribution. Finally, we investigate the effect of grain density, adopting typical values for Earth analog rocks and for meteorites, concluding that for both selections, the final model bulk densities are still in agreement with the observation (Figure 1).

References

[1] Malamud, U. and Prialnik, D. (2015), Modeling Kuiper belt objects Charon, Orcus and Salacia by means of a new equation of state for porous icy bodies, Icarus, 246:21 – 36, Special Issue: The Pluto System on the Eve of New Horizons.

[2] Malamud, U. and Prialnik, D. (2013), Modeling serpentinization: Applied to the early evolution of Enceladus and Mimas, Icarus, 225:763–774.

[3] Kenyon, S. J. and Bromley, B. C. (2012), Coagulation calculations of icy planet formation at 15-150 au: A correlation between the maximum radius and the slope of the size distribution for trans-Neptunian objects, The astronomical Journal, 144:29.

[4] Kenyon, S. J., Bromley, B. C., O'Brien, D. P., and Davis, D. R. (2008), Formation and collisional evolution of Kuiper belt objects, 293–313, University of Arizona Press.

[5] Schubert, G., Hussmann, H., Lainey, V., Matson, D. L., McKinnon, W. B., Sohl, F., Sotin, C., Tobie, G., Turrini, D., and van Hoolst, T. (2010), Evolution of icy satellites, Space Science Reviews, 153:447–484.

[6] Brown, M. E. (2012), The compositions of kuiper belt objects, Annual Review of Earth and Planetary Sciences, 40:467–494.

[7] Yasui, M., and M. Arakawa (2009), Compaction experiments on ice-silica particle mixtures: Implication for residual porosity of small icy bodies, Journal of Geophysical Research (Planets), 114.

EPSC Abstracts
Vol. 10, EPSC2015-750-9, 2015
European Planetary Science Congress 2015

Observations of Chariklo's rings in 2015

B. Sicardy (1), G. Benedetti-Rossi (2), M. W. Buie (3), M. Langlois (4), E. Lellouch (1), J.I.B. Camargo (2), F. Braga-Ribas (5), R. Duffard (6), J.L. Ortiz (6), D. Bérard (1), E. Meza (2), A. Boccaletti (1), D. Bockelée-Morvan (1), C. Dumas (7) and D. Gratadour (1)

(1) LESIA, Observatoire de Paris, CNRS UMR 8109, Université Pierre et Marie Curie, Université Paris- Diderot, 5 place Jules Janssen, F-92195 Meudon Cedex, France (bruno.sicardy@obspm.fr), (2) Observatório Nacional/MCTI, Rua General José Cristino 77, CEP 20921-400 Rio de Janeiro, RJ, Brazil, (3) Southwest Research Institute, 1050 Walnut St., Suite 300, Boulder, CO 80302, USA, (4) CRAL, UMR 5574, CNRS, Université Lyon 1, 9 avenue Charles André, 69561 Saint Genis Laval Cedex, France (5) Federal University of Technology - Paraná (UTFPR / DAFIS), Curitiba, PR, Brazil (6) Instituto de Astrofísica de Andalucía, CSIC, Apartado 3004, 18080 Granada, Spain. (7) European Southern Observatory, Alonso de Córdova 3107, Vitacura, Casilla 19001, Santiago 19, Chile

Abstract

We are organizing several campaigns in 2015 to observe stellar occultations by Chariklo and its rings from the ground. In parallel, three *Hubble Space Telescope* (HST)/WFC3 visits are planned in June and August 2015 to image the system in the near UV and visible, as well as four visits on the *Very large Telescope* (VLT)/SPHERE instrument of the European Southern Observatory (ESO), in the near IR in April and July. Results derived from those observations will be presented.

1. Introduction

A stellar occultation observed on 3 June 2013 revealed the surprising presence of two dense rings around (10199) Chariklo [1], the largest Centaur object known to date with a radius of 119 ± 5 km [2]. This is the first ring system ever detected in the solar system around a body that is not a giant planet.

The two rings (called respectively C1R and C2R) have orbital radii $a_{\rm C1R} = 390.6 \pm 3.3$ km and $a_{\rm C2R} = 404.8 \pm 3.3$ km (1-σ limits), and typical average optical depths of $\tau_{\rm C1R} \sim 0.4$ and $\tau_{\rm C2R} \sim 0.06$. They are separated by a gap of about 9 km that is empty to within an upper limit of $\tau \sim 0.004$.

The rings' changing geometry explains the long term variations of Chariklo's absolute magnitude and the spectral changes observed between 1997 and 2013. They imply a reflectance I/F of about 0.07 for C1R, and show that it contains about 20% of water ice, the latter remaining undetected on Chariklo's surface [3].

An occultation observed in 2014 reveals a W-shaped structure for C1R ring, with the densest parts reaching an apparent optical depth of about 2. The width of C1R may exhibit a m=1 mode, with a width W varying between ∼5.5 and ∼7.1 km over the full 360 degrees longitude range, see Fig. 1 and [4]. The width of C2R is less constrained and lies between 2 and 4 km.

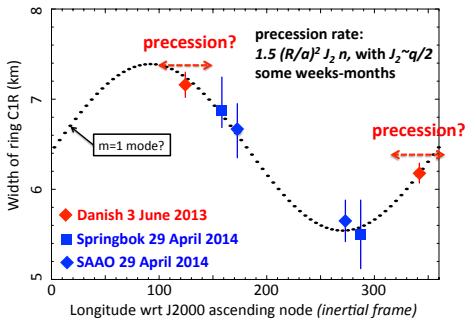

Figure 1: The width of ring C1R as a function of longitude in an inertial reference frame. As the ring precession rate is not known, one cannot conclude at present time if a m=1 mode is present in that ring. From [4].

2. Observations in 2015

Several ground-based stellar occultations by Chariklo are planned for 2015. The main goals of occultations are (1) improve the ring orbital elements, (2) confirm the azimuthal width variation, (3) derive Chariklo's shape (presently unknown) and its orientation relative to the rings, and (4) attempt multi-wavelength observations to detect possible dependence of the optical

depth vs. wavelength, a way to constrain dust particle size distribution, if present.

Similarly, direct imaging of Chariklo and its rings will be performed using HST and VLT.

Three HST visits are planned in 2015 (two in June and one in August), using the WFC3/UVIS camera with filters F300X ($\sim$250-350 nm), F475X ($\sim$400-650 nm) and F350LP ($\sim$300-1000 nm). Dither mode will be applied, resulting in a typical PSF size of about 30 milli-arcsec (mas), corresponding to about 300 km at Chariklo.

Meanwhile, four visits are planned (one in April, three in July) using the new SPHERE high contrast instrument of the VLT/ESO in the near IR (Y, J and H bands), with typical expected PSF sizes of 30-40 mas (300-400 km at Chariklo)

The aims of the HST and VLT imaging campaigns are: (1) obtain direct images of the rings, confirming their existence and their orientation, (2) derive multi-wavelength photometry, thus constraining their composition (concerning in particular the presence of water ice), (3) perform a deep search of small satellites (down to a few km in diameter) and (4) faint dusty rings around Chariklo (down to about $\tau \sim 10^{-5}$-10^{-6}), and (5) search possible cometary jets or coma, akin to what is observed around another Centaur, Chiron.

First results will be presented at the meeting, as observations have not yet been performed at the moment of writing this abstract.

Acknowledgements

The authors acknowledge support from the French ANR grant 11-IS56-0002 'Beyond Neptune II' (Programme Blanc International).

References

[1] Braga-Ribas, F., Sicardy, B., Ortiz, J. L., Snodgrass, C., Roques, F. *et al.*: A ring system detected around the Centaur (10199) Chariklo, Nature, Vol. 508, pp. 72-75, 2014.

[2] Fornasier, S., Lazzaro, D., Alvarez-Candal, A., Snodgrass4, C., Tozzi, G. P. *et al.*: The Centaur 10199 Chariklo: investigation into rotational period, absolute magnitude, and cometary activity, Astron. Astrophys., Vol. 568, L11, 2014.

[3] Duffard, R., Pinilla-Alonso, N., Ortiz, J.L., Alvarez-Candal, A., Sicardy, B. *et al.*: Photometric and spectroscopic evidence for a dense ring system around Centaur Chariklo, Astron. Astrophys., Vol. 568, A79, 2014.

[4] Sicardy, B., Braga-Ribas, F., Ortiz, J.L., Vieira-Martins, R., Colas, F. *et al.*: Dense and narrow rings around the Centaur object (10199) Chariklo, $46^{\rm th}$ annual meeting of the Division for Planetary Sciences, 9–14 November 2014, Tucson, USA, 2014.

EPSC Abstracts
Vol. 10, EPSC2015-845, 2015
European Planetary Science Congress 2015

RECON – A new system for probing the outer solar system with stellar occultations

M. W. Buie (1), J. M. Keller (2) and L. H. Wasserman (3)
(1) Southwest Research Institute, Boulder, Colorado, USA, (2) CalPoly, San Luis Obispo, California, USA, (3) Lowell Observatory, Flagstaff, Arizona, USA. (buie@boulder.swri.edu)

Abstract

The Research and Education Collaborative Occultation Network (RECON) is a new system for coordinated occultation observations of outer solar system objects. Occultations by objects in the outer solar system are more difficult to predict due to their large distance and limited duration of the astrometric data used to determine their orbits and positions. This project brings together the research and educational community into a unique citizen-science partnership to overcome the difficulties of observing these distant objects. The goal of the project is to get sizes and shapes for TNOs with diameters larger than 100 km. As a result of the system design it will also serve as a probe for binary systems with spatial separations too small to be resolved directly. Our system takes the new approach of setting up a large number of fixed observing stations and letting the shadows come to the network. The nominal spacing of the stations is 50 km. The spread of the network is roughly 2000 km along a roughly north-south line in the western United States. The network contains 56 stations that are committed to the project and we get additional ad hoc support from the International Occultation Timing Association. At our minimum size, two stations will record an event while the other stations will be probing for secondary events. Larger objects will get more chords and will allow determination of shape profiles. The stations are almost exclusively sited and associated with schools, usually at the 9-12 grade level. We have successfully completed our first TNO observation which is presented in the compainion paper by G. Rossi et al (this conference).

1. Introduction

The normal methodology used for many decades in the occultation community is to strive for a ground-track prediction of the shadow path that is accurate enough to permit placing mobile stations in the shadow. This method imposes a requirement that the prediction of the relative position of the star and occulting body be known on a scale comparable to the size of the body. Meeting this requirement is not difficult for main-belt asteroids (MBAs). At 1 AU, the scale on the plane of the sky is 725 km/arcsec. Using a notional size of D=100 km (roughly $H_V = 9$) at a geocentric distance of 1 AU, a differential astrometric precision of 0.14 arcsec will produce a prediction where the error is equal to the size of the object. The astrometric precision required gets linearly smaller with increasing geocentric distance. Thus, a TNO at 40 AU would require a precision of ∼4 mas to get the same predictive knowledge of the ground-track. Getting such an accurate prediction can be done but is at the level of the best ever done and requires a substantial effort on large telescopes for each prediction.

By increasing the size of the network we relax the requirements on the astrometric precision needed for a successful observation. Figure 1 shows a map of the network of communities in the western United States that have been recruited and trained to collect occultation lightcurve data. One consequence of this design is that few stations will see any event but all stations will probe for additional material near the primary object. This system will be especially powerful for providing constraints on very close binaries and rings.

2. Instrumentation

The standard equipment provided is an 28-cm computer-controlled alt/az telescope (Celestron CPC1100). This system is very easy to assemble and align to the sky. Once aligned, the system can point to a desired target to a region just a little larger than the camera FOV. The video camera is made by MallinCAM and is specially designed to permit integrating on the target up to 2.1 seconds while maintaining a standard NTSC video signal. Timing data is provided by the IOTA-VTI GPS-based unit that superimposed time information on the video coming

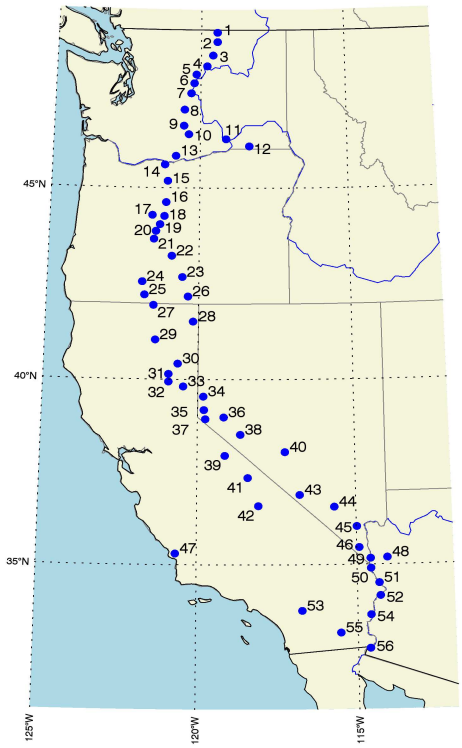

Figure 1: Map of the RECON sites.

from the camera. The data are collected on a small laptop computer with a video frame grabber. All of the equipment, except for the laptop, is powered from an external 12V battery pack. The combined cost of a single station is roughly $5000. This system can collect useful data on stars as faint as R=16.5.

3. Predictions

To support the project, we are building an automated TNO occultation prediction system. The system looks for events anywhere on the Earth but also generates special topocentric supporting information for events within reach of RECON. All of these predictions are to be made public to encourage participation from other un-affilated teams. Many of the targets we are chasing are rather faint, requiring special effort to collect additional astrometry with 4-m class telescopes. Most of the recent successes with TNO occultations have largely been for objects within reach of 2-m class telescopes.

4. Observations to Date

Observations by RECON began in May 2012 with the pilot team sites. Nearly 40 events, mostly with main-belt asteroids, were attempted and most were successful. Included these observations were participation in a campaign on Jupiter Trojan Patroclus[1]. Our first TNO event was in Nov 2014 of (229762) 2007 UK_{126} (see presentation by G. Rossi).

5. Summary and Conclusions

This new system wasfully implemented with the completion of training in April 2015 and is now ready to begin its exploration of the Kuiper Belt. The project is funded through 2019. Stastistical predictions suggest we will be able to get successful observations of 1-2 TNOs per year, including prediction uncertainties and losses due to weather. These data will provide new measurements of sizes of smaller TNOs and contrain the population of ultra-tight binaries in this primoridal population.

Acknowledgements

We thank the hundreds of team members for the RECON network and all their students for their dedication to the project. Funding for this work was provided by the United States National Sciencce Foundation. We also thank the amateur community, largely represented by IOTA (International Occultation Timing Association), for their perseverence, inventiveness, and dedication to all things related to occultations.

References

[1] Buie, M.W., Olkin, C.B., Merline, W.J. *et al.*: Size and Shape from Stellar Occultation Observations of the Double Jupiter Trojan Patroclus and Menoetius, Astron. J. vol 149, p. 113, 2015.

EPSC Abstracts
Vol. 10, EPSC2015-899, 2015
European Planetary Science Congress 2015

Pluto's Atmosphere at the Time of the New Horizons Flyby from the 29-JUN-2015 Occultation

E.Young (1), M. Skrutskie (2), L. Wasserman (3), R. Howell (4) and the PHOT team
(1) Southwest Research Institute, Boulder, CO 80302, USA (efy@boulder.swri.edu / Fax: +1-303-546-9687), (2) University of Virginia, (3) Lowell Observatory, (4) University of Wyoming

Abstract

Pluto is expected to occult a star on 29-JUN-2015, only two weeks before the scheduled New Horizons flyby on Pluto on 14-JUL-2015. This occultation should be remarkable for several reasons in addition to its synergy with the spacecraft observations. First, the occulted star is by far the brightest ever to be observed in a Pluto occultation: its V-mag is 12.10 $\pm$ 0.03, about ten times brighter than Pluto itself. We are deploying a wide array of telescopes to obtain quality lightcurves at 10 Hz, sufficient to resolve vertical atmospheric structure (e.g., gravity waves) at the 2.5-km scale over a range of radii from about 1195 to 1300 km. Second, we plan to obtain lighcurves in infrared wavelengths near 1.7 μm, where the star's H-mag (about 11) is bright enough to provide useful signal-to-noise ratios, albeit at slower cadences near 1 Hz (about two points per scale height). The combination of simultaneous IR and visible wavelength lightcurves should address the decades-old question: is there haze in Pluto's atmosphere, and if so, what is its opacity? New Horizons should image haze layers in reflected light as the occultation quantifies haze extinction in transmitted light: the combination could potentially let us solve for haze phase functions. Third, the current predicted shadow path is centered over much of New Zealand. We plan to deploy three portable telescopes in New Zealand to locations that are candidates for observing central flashes. If successful, these lightcurves can tell us (a) the oblateness of Pluto's atmosphere and (b) the detailed density gradient profile at radii near 1215 km, which (in turn) is a function of trace abundances of CO and CH_4 a few tens of km above Pluto's surface.

We will report on lightcurves obtained on 29-JUN-2015, the column abundance of Pluto's atmosphere just two weeks before the New Horizons flyby, the detection (or not) of haze, and – if central flashes are obtained – the oblateness of Pluto's atmosphere.

1. Figures

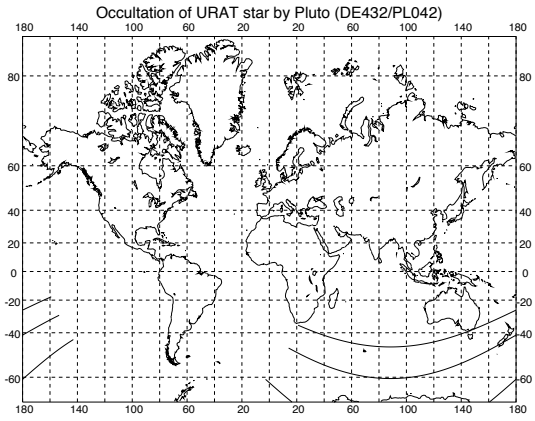

Figure 1: Our current prediction (circa 6-MAY-2015) for the stellar occultation by Pluto on 29-JUN-2015. Continental Australia is a nominal miss at this point, Tasmania should see positive lightcurves, possibly grazing events, and New Zealand should provide central flash lightcurves. The N/S errors on this prediction are approximately 11 mas, or about 280 km.